Electrochimica Acta 456 (2023) 142469

Contents lists available at ScienceDirect

Electrochimica Acta

journal homepage: www.journals.elsevier.com/electrochimica-acta

Solvent-free lithium iron phosphate cathode fabrication with fibrillation of polytetrafluoroethylene

Yang Zhang [a,b], Song Lu [a], Fengliu Lou [b,*], Zhixin Yu [a,c,*]

[a] Department of Energy and Petroleum Engineering, University of Stavanger, 4036 Stavanger, Norway
[b] Beyonder AS, 4313 Sandnes, Norway
[c] Institute of New Energy, School of Chemistry and Chemical Engineering, Shaoxing University, Shaoxing 312000, China

ARTICLE INFO

Keywords:
Solvent-free
Electrode fabrication
LFP
PTFE fibrillation

ABSTRACT

Fabricating electrode for lithium-ion batteries (LiBs) with solvent-free (SF) procedure can save energy and improve electrochemical performance simultaneously. Polymer fibrillation is one of the most promising SF procedures due to its feasibility for upscale production. The hardness of lithium iron phosphate (LFP) impedes its SF fabrication with polytetrafluoroethylene (PTFE) fibrillation. In this study, we successfully expanded PTFE fibrillation for SF LFP electrode fabrication with the help of carbon nanotubes (CNTs). CNTs increase the conductivity of electrode, and act as matrix for LFP particles to ensure relative displacement to further fibrillate PTFE to form self-supporting electrode film when the dry mixture was hot rolled. The SF LFP/hard carbon full cells were fabricated and demonstrated comparable electrochemical performance to slurry casting (SC) fabricated LFP electrode. The initial coulombic efficiency (ICE) of full cell increased to more than 95% after prelithiation.

1. Introduction

Lithium-ion batteries (LiBs) dominate consumer electronics for their high energy density, long cycle life, high power and good reliability [1]. Recently, LiBs are gaining even more attention owing to the specific energy improvement and cost reduction, especially in transportation sector [2,3]. Replacing internal combustion engine with energy storage devices such as batteries is critical to reduce CO_2 emission and alleviate climate change [4]. However, the high cost and limited energy density of current commercial LiBs impede widespread deployment of LiBs in electric vehicles (EVs) [5]. The cost of LiBs is mainly ascribed to raw materials and manufacturing cost, which are determined by the electrode manufacturing process [6]. At present, electrodes of commercial LiBs are fabricated by the so-called slurry casting (SC) procedure, where active material, conductive additives and polymer binder are mixed in solvent, e.g., water for anode and N-methyl-2-pyrrolidone (NMP) for cathode to form slurry with appropriate viscosity [7,8]. The slurry is subsequently cast onto substrate, e.g., copper foil for anode and aluminum foil for cathode, and dried with the coating machine. The drying process is complicated with dozens of meters long ovens under high temperature consuming huge amount of energy [7,9]. In addition, uneven binder distribution resulting from binder floating with quick solvent evaporation during drying limits the fabrication of thick electrode. The toxicity of NMP for SC cathode fabrication is also an issue, because organic solvent leakage is inevitable even with complicated and expensive NMP recovery systems [10].

Fabricating electrode without solvent to avoid the drying process can save much energy and improve the energy density of the LiBs simultaneously with the adoption of high active material loading design. There are many different solvent-free (SF) procedures for electrode fabrication including dry powder deposition, polymer fibrillation, chemical or physical vapor deposition, 3 D printing, melting and extrusion, direct pressing [11]. Polymer fibrillation is one of the most promising SF procedures when taking upscale production into consideration. Fibrillation under high shear force makes polytetrafluoroethylene (PTFE) the most-often used polymer for fibrillation-based SF electrode fabrication, especially for activated carbon electrode. The lowest unoccupied molecular orbit (LUMO) of PTFE is not only lower than common polymer binders such as polyvinylidene fluoride (PVDF) and carboxymethyl cellulose (CMC), but also lower than common solvent like ethylene carbonate (EC) used in electrolyte. The low LUMO of PTFE allows it to accept electrons and get reduced [12]. We have previously succeeded in applying PTFE fibrillation for SF hard carbon and graphite anode fabrication, even though PTFE is unstable in anode [13]. SF procedure is

* Corresponding author.
E-mail addresses: fengliu@beyonder.no (F. Lou), zhixin.yu@uis.no (Z. Yu).

https://doi.org/10.1016/j.electacta.2023.142469
Received 7 March 2023; Received in revised form 4 April 2023; Accepted 24 April 2023
Available online 24 April 2023
0013-4686/© 2023 The Authors. Published by Elsevier Ltd. This is an open access article under the CC BY license (http://creativecommons.org/licenses/by/4.0/).

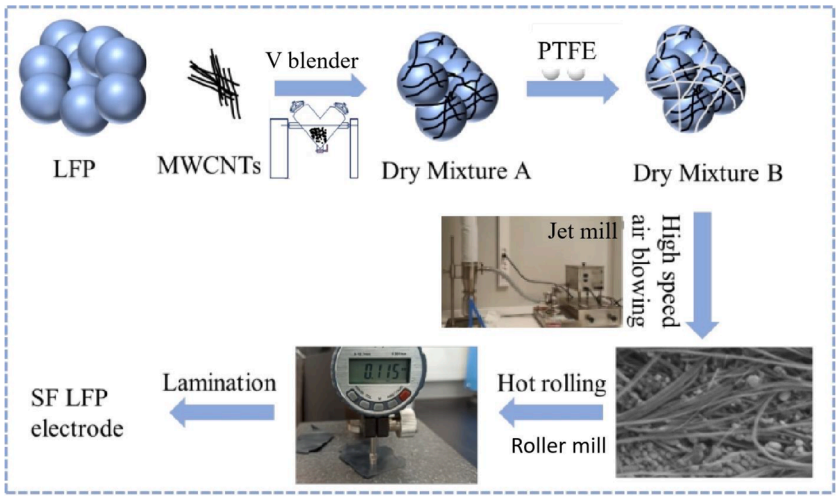

Fig. 1. Schematic diagram of SF LFP electrode fabrication based on PTFE fibrillation, including dry mixing, fibrillation, hot-rolling and lamination.

also promising for non-porous electrode fabrication for all-solid-state-batteries (ASSBs), since most solid electrolytes (SEs) are sensitive to moisture and polar solvents [11]. Maxwell company have successfully fabricated lithium nickel manganese cobalt oxide (NMC)/graphite LiBs based on PTFE fibrillation [14]. SF NMC/graphite cells exhibited high-rate capability and decent cycle life with high mass loading. Good electrochemical performance and roll-to-roll manufacturing process make the procedure compatible with current commercial LiBs production line. Hippauf et al. applied the SF procedure for NMC electrode fabrication with 0.1% PTFE, the content of which is the lowest ever reported [15]. However, the limited reserves, unbalanced distribution and high cost of metals especially cobalt make NMC based LiBs unsustainable. On the contrary, lithium iron phosphate (LFP) is much cheaper with longer cycle life and better safety, but with low specific energy and poor rate performance [16,17]. As new structures like cell to pack (CTP) and cell to chassis (CTC) are being developed, the system integration degree of battery pack increases a lot and LFP is becoming increasingly attractive [18,19].

SF procedure is well suited for LFP electrode fabrication. On the one hand, spot contact between PTFE fibrils and LPF particles facilitates ion transportation to increase the rate performance. On the other hand, adoption of thick LFP electrode can increase the specific energy of LFP cells. However, the PTFE fibrillation procedure is not preferable for LFP electrode fabrication due to the hardness of LFP particles and smaller particle size, requiring large amounts of additives to make the self-supporting LFP electrode film. For example, 40% activated carbon was added to increase the flexibility of the LFP electrode when PTFE was used for LPF electrode fabrication [20]. Therefore, there are still great challenges associated with fabricating LFP electrodes with low cost and good performance through PTFE fibrillation.

In this study, we for the first time successfully fabricated LFP electrode for LiBs with PTFE fibrillation using carbon nanotubes (CNTs) as additive. The CNTs can increase the conductivity of the electrode as well as act as matrix to hold LFP particles, where PTFE powders are further fibrillated to ensure the formation of self-supporting LPF electrode film during the hot rolling process. SF LFP/hard carbon full cells were fabricated successfully and demonstrated good stability. With the help of prelithiation, the initial coulombic efficiency (ICE) of SF LFP/hard carbon cells were increased to 95%. The SF LFP/hard carbon full cells also demonstrated decent stability with more than 95% capacity retention after 50 cycles under the current of 0.5C in coin cells. The electrodes are fabricated through roll-to-roll process, which is compatible with the current LiBs production line, making the method promising to replace the SC procedure for commercial LiBs.

2. Experimental

2.1. Electrodes fabrication

Fig. 1 showed schematically the procedure of SF LFP cathode fabrication with PTFE fibrillation. Different carbon materials such as activated carbon (Fujian Yuanli, China), carbon black (MTI, China), conducting graphite (Shanshan, China) and CNT (Sigma-aldrich, Germany) has been used as additives for SF cathode fabrication. Use CNT as an example, LFP (Shanshan, China), CNT and PTFE powder (MTI, China) were used directly for electrode fabrication. Typically, a powder mixture was prepared by mixing LFP and CNT in a conical mixer at a speed of 1400 r/min for 60 min. After that, PTFE powder was added to the mixture and mixed for another 20 min using a V blender. High-speed dry air was then applied using a 2-inch grinding chamber jet mill (Sturtevant, USA) to fibrillate PTFE to cotton candy like dry mixture. The free-standing electrode film was formed when the dry mixture was hot rolled at 160 °C using a calendering machine at a speed of 15 cm/min. The thickness of the electrode film was adjusted according to the gap between rolls of calendering machine and the times the electrode film going through the rolls. Finally, the free-standing film was laminated onto a 13 μm thick carbon coated aluminum foil (Nanoblue, China) using hot rolling at 80 °C.

FTFE film was fabricated to confirm their stability in cathode. For PTFE film fabrication, 80% carbon black was added to increase the electronic conductivity. The PTFE powder and carbon black were mixed for 30 min in a kitchen mixer, then the mixture was ground using an agate mortar until the formation of flake. Finally, the flake was hot rolled using a calendering machine.

To compare the performance of SF LFP electrode, SC LFP electrode was also fabricated. LFP, PVDF and CNTs were mixed in NMP with the same mass ratio. The slurry was cast onto the Al foil and dried. The SC LFP was subsequently calendered with the specific capacity of 1.6 mAh/cm^2.

2.2. Cell assembly

Both half cells and full cells were assembled with 2032-coin cell parts (MTI, China) in an argon-filled glove box, where water and oxygen concentrations were less than 0.01 ppm. For half cells, two layers cellulose film (Celgard, USA), lithium foil (Sigma-Aldrich, 600 μm, Germany) and 50 μL 1.2 M $LiPF_6$ in EC-EMC (3/7, v/v) with 10 wt.% fluoroethylene carbonate (FEC) were used as separator, counter electrode and electrolyte, respectively.

For full cell assembly, SF hard carbon electrodes were used as anode.

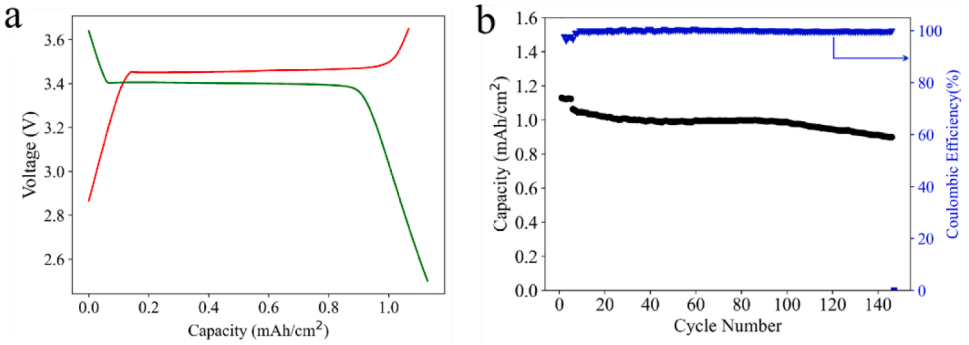

Fig. 2. (a) Capacity-voltage curves for SF LFP-AC half cells; (b) Stability of SF LFP-AC half cells under the current of 1.2 mA/cm^2.

SF hard carbon electrode was fabricated with a similar method in our previous study with the weight ratio of hard carbon/carbon black/PTFE/PVDF of 90/5/3/2 [13,21]. The thickness of SF hard carbon electrode was 120 μm with the capacity of 3.7 mA/cm^2. The capacity ratio of anode to cathode (N/P ratio) was set to be 1.2: 1.

2.3. Prelithiation

Single layer SF hard carbon electrode with a dimension of 5 × 5 cm was assembled into monolayer pouch cell with lithium foil as counter electrode. The separator and electrolyte were similar as these used in coin cells. The pouch cell was discharged under the current of 0.3 mA/cm^2 with the lithiation capacity of 3 mAh/cm^2. The pouch cell was disassembled in glovebox and the prelithiated hard carbon electrode was washed with dimethyl carbonate (DMC) and dried under room temperature overnight in glovebox. The prelithiated hard carbon electrode was further assembled with SF LFP electrode to obtain full SF LFP/hard carbon cell.

2.4. Electrochemical test and electrode characterization

The galvanostatic charge/discharge tests were performed under room temperature using an 8-channel battery analyzer (Neware, China). The cutoff voltage was between 2.5 to 3.65 V for half cells. All cells were aged under room temperature for 12 h before testing and underwent several formation cycles. Cyclic voltammetry (CV) was carried out in the voltage range of 2–3.8 V at a scanning rate of 0.5 mV/s.

The pristine and cycled electrodes were characterized using a scanning electron microscope (SEM, Phenomenon LE). The cycled electrodes were charged to the fully delithiation state after cell cycling, followed by disassembling the cell, dipping the electrode into DMC solution for 2 h to remove any residual electrolyte, and drying at room temperature overnight in an argon filled glove box for further analysis. X-ray diffraction (XRD) characterization was conducted with a X'Pert PRO MPD instrument. X-ray photoelectron spectroscopy (XPS) study with conducted with a Thermo Kalpha instrument.

3. Results and discussion

3.1. Stability of PTFE in cathode

PTFE has been shown to be instable in anode, while its stability in cathode is waiting for further clarification [21]. PTFE film was prepared and coin cells were assembled with PTFE film as cathode and lithium foil as counter electrode. The charge/discharge testing was conducted between 2–4 V under the current of 1 mA/cm^2. The capacity of PTFE film is only 1.5 mAh/g, which is ascribed to the capacitance of carbon black (Figure S1a in Supporting Information). The negligible capacity of PTFE demonstrated its stability within 2–4 V.

XRD characterization was conducted on both pristine and cycled PTFE film. The characteristic peak of PTFE at around 19° remained after lithiation, as shown in Figure S1b. SEM characterization of the pristine and cycled PTFE film showed that after three charge/discharge cycling, the PTFE fibrils maintained their structure (Figure S1c and d). The results from electrochemical capacity, XRD and morphology study consistently demonstrated that PTFE is stable in cathode.

3.2. SF LFP-AC electrode

PTFE fibrillation has been used for NMC electrode fabrication for both LiBs and ASSBs. However, there is no PTFE fibrillation based LFP electrode for LiBs so far. We first tried LFP electrode fabrication with the weight ratio of LFP/activated carbon/PTFE = 47.5/47.5/5. Activated carbon was added to increase the flexibility of electrode. The SF LFP-AC electrode was prepared according to the procedure described in Section 2.1. Thereafter, coin cells were assembled with lithium foil as counter electrode and cycled under the current of 1C. The capacity-voltage curves have the mixing characteristics of capacitors and batteries with the specific capacity of 1.1 mAh/cm^2 (Fig. 2a). The voltage increases linearly with capacity within 2–3.4 V, resulting from capacitance of activated carbon. After that, a charge plateau appears at 3.45 V, which is ascribed to the Faradaic reaction of LFP. The half cells have good stability with 90% capacity retention after 100 charge/discharge cycling (Fig. 2b). After 100 cycles, the capacity fade speed accelerates. The coin cell was then disassembled, and the electrode and separator were dry without obvious electrolyte observed. The fast capacity fade could be attributed to electrolyte consumption since only 50 μm electrolyte was injected in the coin cell.

The PTFE fibrils could be observed on the surface of pristine LFP-AC electrode under SEM, as shown in Figure S2a and b. Activated carbon acts as conductive additive to maintain the good conductivity network of the electrode to ensure good performance of SF LFP-AC electrode under high current (Figure S2c). However, activated carbon has low density and large specific surface area, which will result in low specific energy and moisture absorption. For LFP-AC electrodes, the tap density of activated carbon (0.67 g/cm^3) is much smaller than LPF (1.3 g/cm^3). With 47.5% percent of activated carbon, the volume of activated carbon is much greater than LPF. The compressed density of LFP-AC electrode is only 1.6 g/cm^3, significantly lower than LFP electrodes (2.1–2.2 g/cm^3). The activated carbon acts as matrix to provide relative opposite motion of PTFE and roll when the dry mixture was compressed under calendering machine. Consequently, SF LFP could be fabricated successfully with the addition of activated carbon, but the compressed density is too low.

3.3. Carbon additive material screening

To fabricate SF LFP electrode with less additive and higher compressed density, we tried SF LFP electrode fabrication with different carbon materials including carbon black, conductive graphite, and CNT.

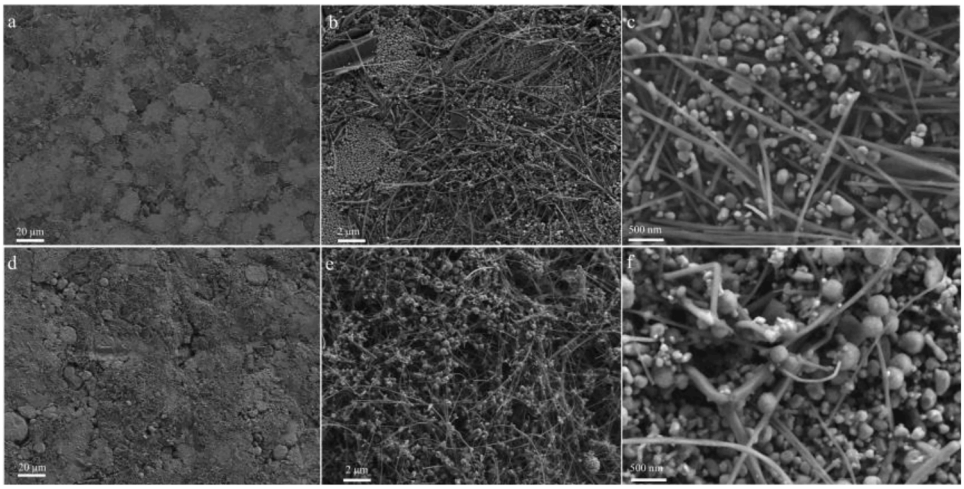

Fig. 3. SEM images of pristine SF LFP electrode (5% CNTs) with different magnification. (a) x1000; (b) x5000; (c) x10000; SEM images of SF LFP electrode (5% CNTs) after 50 cycles. (d) x1000; (e) x5000; (f) x10000.

The content of different carbon materials were screened with various mass ratio of LFP/carbon materials/PTFE, as summarized in Table S1. The key parameter for carbon materials to assist LFP electrode film formation is the tap density. The tap density of carbon black, conductive graphite and CNT are 0.16, 0.96 and 0.025 g/cm^3, respectively.

When the carbon black ratio is 10%, a mixture of LFP/carbon black/PTFE (85/10/5 wt.%) was hot rolled under the same condition as the LFP-AC electrode. Out of our expectation, the rolls were stuck by the dry mixture powder. To form self-supporting electrode film, further fibrillation of PTFE is necessary when the mixture was compressed through the calendering rolls. The hardness of LFP particles prevent the tangent motion of calendering roll to PTFE particles, failing to further fibrillate PTFE. When increase carbon black to 20%, self-supporting LFP electrode film with some cracks could be formed. Flexible LFP electrode film was possible to be fabricated when carbon black was further increased to 40%. Graphite itself is a soft material, however, no LFP electrode film could be formed even when graphite was increased to 40%. Therefore, the relative high tap density of carbon black and conductive graphite make them insufficient to offer shear force during hot rolling. Self-supporting LFP electrode film could be formed with only 5% CNT. CNT has more relative volume ratio at the same weight ratio due to its low tap density. The minimum amount of different carbon materials as additives required for LFP film formation was listed in Table S1. The lower the tap density of carbon material, the less carbon material required to form LFP film. Subsequently, we will only focus on SF LFP electrode fabrication with CNTs.

The mechanical strength of electrode film, which is critical for up-scale production, is determined by the fibrillation degree of PTFE powder. The temperature has huge effect on the property of PTFE [22, 23]. The PTFE has a well-ordered triclinic crystal structure below 19 °C,

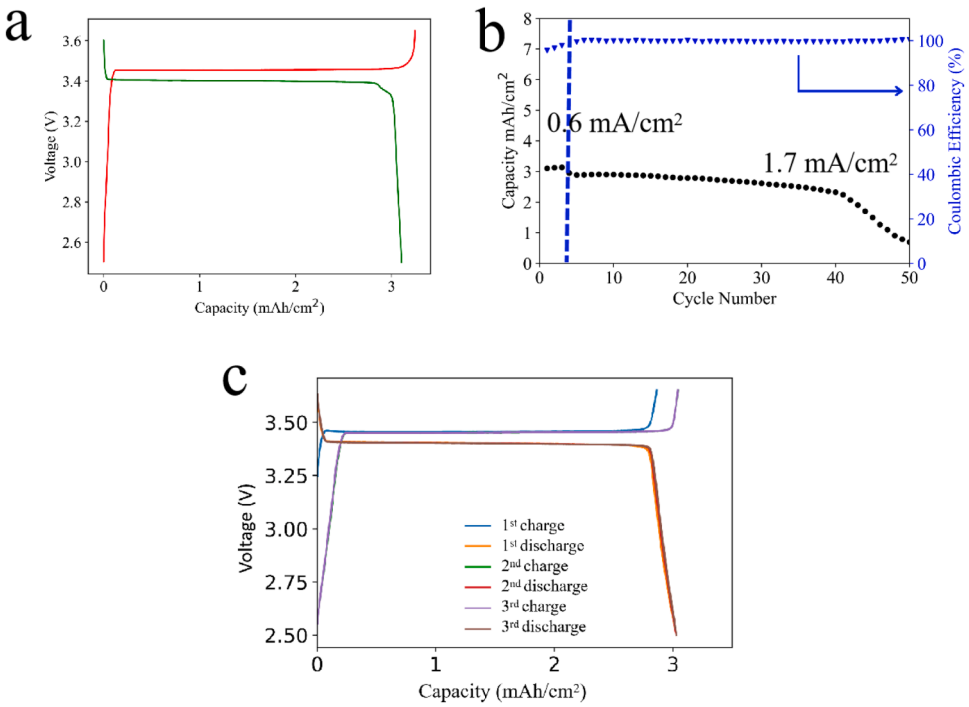

Fig. 4. (a) Capacity-voltage curves for SF LFP half cells; (b) Stability of SF LFP half cells under the current of 1.7 mA/cm^2; (c) Capacity recovery of cycled SF LFP electrode when it was reassembled with fresh lithium foil.

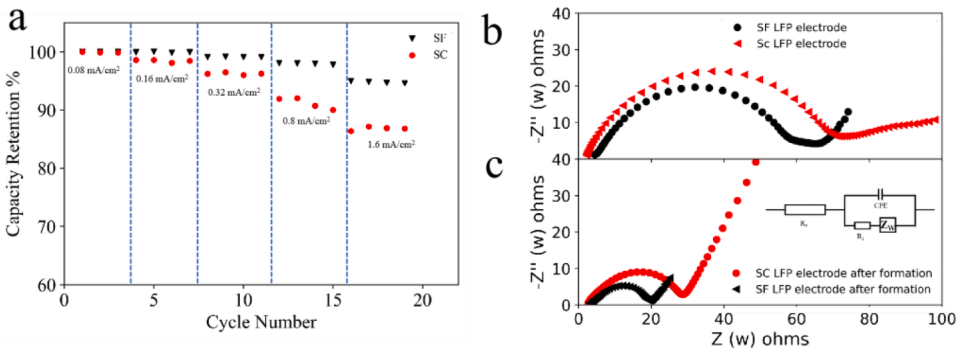

Fig. 5. (a) Rate performance for SF and SC LFP electrode under different current density; (b) EIS comparison between pristine SF and SC LFP electrodes in half cells; (c) EIS comparison between SF and SC LFP electrodes after formation in half cell.

the hard PTFE particles will slide past each other when shear force was applied without being fibrillated. Between 19 to 30 °C, the crystalline PTFE turns into hexagonal phase. Further heating PTFE to higher temperature will convert it into a disordered pseudo-hexagonal phase with molecule chain packed loosely. The higher the temperature, the easier the PTFE will be fibrillated before reaching its melting point. To get the optimal mechanical strength of electrode film, temperature was screened between 40 and 160 °C during hot rolling. It turned out that the electrode film cannot be formed below 90 °C. The tensile strength of the obtained electrode film increased with temperature between 100 and 160 °C. The thickness of electrode film was reduced to 125 μm after pressing several times. The compressed density of the electrode film was 2.0 g/cm^3, which is similar as the commercial LFP electrode (2.1–2.2 g/cm^3). The electrode film was subsequently laminated onto carbon coated aluminum foil.

PTFE fibrils were observed from fresh LFP electrode, demonstrating good fibrillation of PTFE (Fig. 3a). LFP powders were distributed in the matrix of 5% CNT (Fig. 3b and c), enabling good conductivity and mechanical strength of the electrode. PTFE fibrils were more visible from the cross-sectional images, as shown in Figure S3a and b. EDS-mapping of pristine LFP electrode in Figure S3c demonstrated the uniform distribution of PTFE, which guarantees good mechanical strength of the electrode film.

3.4. SF vs. SC LFP electrodes

The cycling stability of SF LFP electrode was studied in half cells with specific capacity of 3.1 mAh/cm^2. Fig. 4a shows that LFP delivered a capacity of 142 mAh/g under the current of 0.6 mA/cm^2 with ICE of 95.6%, which is similar to commercial LFP electrode at room temperature. The capacity retention was 80% after 40 charge/discharge cycles under a current of 1.7 mA/cm^2 (Fig. 4b). However, after 40 cycles, the capacity faded very fast. When the coin cells were disassembled, there was no obvious cracks from the LFP electrode, while the electrode and separator were dry and the lithium electrode was pulverized. Therefore, the fast capacity fading was mainly caused by the pulverization of lithium foil and electrolyte consumption. SEM characterization of the cycled LFP electrode showed that the structure of LFP electrode was well maintained (Fig. 3d-f), and the cross-section observation and EDS mapping of the cycled electrode were also similar as the pristine SF LFP electrode (Figure S3d-f).

The cycled SF LFP electrodes were assembled with fresh lithium foil and separator into coin cells and the capacity recovered to more than 95% of the initial capacity. There are no obvious capacity fading during first several cycling, as shown in Fig. 4c. The results demonstrated the good stability of SF LFP electrode even under high loading and current density.

LFP electrodes were also fabricated through SC procedure for comparison. It is worth mentioning is that the material loading of SC procedure is 11.5 mg/cm^2 (1.6 mAh/cm^2), which was much smaller than that of SF LPF electrode. When we try to increase the loading of SC electrode, cracks appeared after compressing. In contrast to SF LFP electrode, the SC LFP electrode delivered a specific capacity of 138 mAh/g under the same current density. To further compare the rate capability of the two different electrodes, the capacity was tested under different current density from 0.08 to 1.6 mA/cm^2. Fig. 5a shows that the SF LFP electrodes exhibited higher rate capability performance than the SC LFP electrode. The capacity retention for SF electrode was 99.8, 99.1, 98.1, 95.0% under 0.16, 0.32, 0.8, 1.6 mA/cm^2, while the capacity retention for SC electrode was 98.6, 96.2, 91.7, 87.1% under the same current density.

Electrochemical impedance spectroscope (EIS) analysis was conducted to further explain the different performance of SF and SC LFP electrodes. The EIS date was fitted using python impedance package, with the equivalent circuit = R_0 - p(R_1, CPE_1) - Z_w, where R_0 and R_1 refer to ohmic and charge transfer resistance, while CPE_1 and Z_w are constant phase element and Warburg coefficient, respectively. The ohmic and charge transfer resistance for the SF LFP electrode after formation were calculated to be 3.4 and 15.4 ohms, while they were 3.7 and 17.6 ohms for the SC LFP electrodes. For both pristine electrodes and electrodes after formation, the charge transfer resistances of SC electrodes are larger than SF LFP electrodes, as shown in Fig. 5b and c. The EIS results were consistent with their rate performance. The different binding mechanism of PTFE fibrillation-based SF procedure facilitates better rate performance, where the spot contact of PTFE fibrils and LFP particles is beneficial for charger transfer and good rate capability. For electrode made from SC procedure, PVDF was first dissolved in NMP and formed a compact insulating layer around LFP particles, which is detrimental for charge transfer.

3.5. SF hard carbon/LFP full cell

Hard carbon has low volume variation during charge/discharge process, ensuring longer cycling life than graphite electrode [24,25]. We have demonstrated earlier that PTFE fibrillation-based SF hard carbon electrode had good stability [21]. Full cells were assembled with SF hard carbon electrodes and SF LFP electrodes. The SF hard carbon electrode was fabricated with a similar procedure reported earlier, where 2% of PVDF and 3% PTFE were used as binders [13]. The N/P ratio of the full cell was set to 1.2, and the areal capacity of hard carbon and LFP electrodes were 3.7 and 3.1 mAh/cm^2, respectively. Hard carbon has low ICE, which impedes its application in commercial LiBs [26,27]. The reaction between PTFE and lithium ion during the first lithiation process make the ICE even lower. However, with the help of prelithiation, we can alleviate the low ICE issue, and the ICE is adjustable by the extent of prelithiation. For prelithiation, single layer pouch cells were assembled with lithium foil as counter electrode. The hard carbon electrode was lithiated with the capacity of 2 mA/cm^2. The prelithiated SF hard carbon

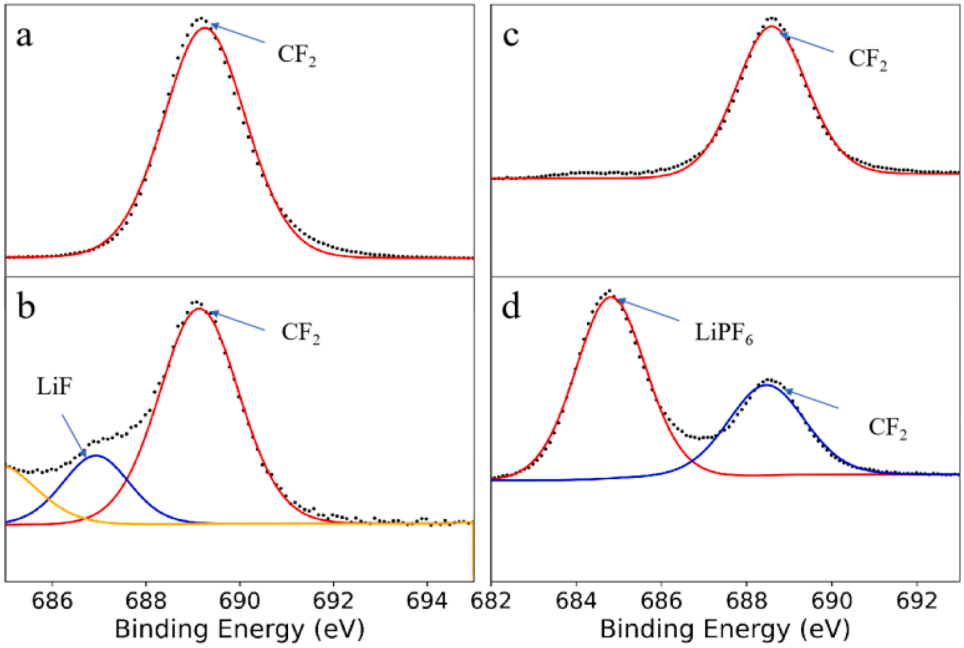

Fig. 6. XPS analysis of F 1 s for different electrodes (a) pristine SF hard carbon electrode, (b) prelithiated SF hard carbon electrode, (c) pristine SF LFP electrode, (d) cycled SF LFP electrode.

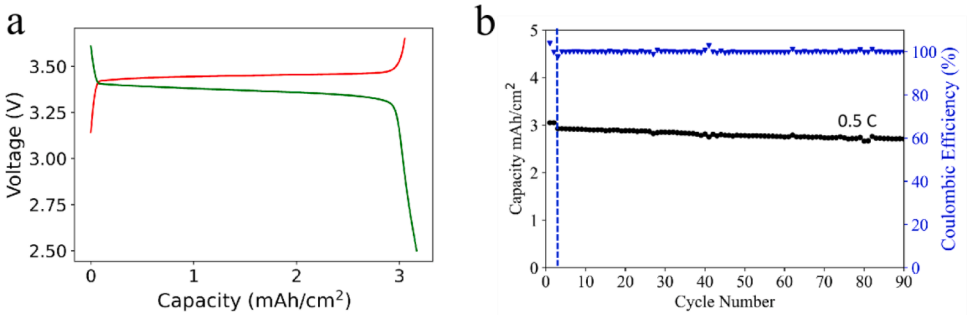

Fig. 7. (a) Capacity-voltage curves for SF LFP/hard carbon cells; (b) Stability of SF LFP/hard carbon cells under 0.5C.

electrode was assembled into full coin cells with SF LFP electrode as cathode.

Pristine and prelithiated hard carbon electrodes was characterized with SEM from both top and cross-sectional view, as shown in Figure S4 and Figure S5. PTFE fibrils tie up hard carbon particles together to form compact structure (Figure S4a-c, Figure S5a and b). After lithiation, most of PTFE fibrils decomposed (Figure S4d-f), but the electrodes kept their integrity with the help of PVDF (Figure S5d and e). EDS mapping in Figure S5c and f showed that there was no significant difference between the fluorine distribution for pristine and lithiated hard carbon electrode, demonstrating good stability of SF hard carbon electrode during prelithiation.

XPS analysis was conducted to monitor PTFE decomposition from SF hard carbon and SF LFP electrodes. Fig. 6a shows the F 1 s peak at 689.2 eV in pristine hard carbon electrode, which was attributed to CF_2. After lithiation, new peak appeared at 686.9 eV, which was ascribed to LiF from the decomposition PTFE (Fig. 6b). The same peak from PTFE appears in SF LFP electrode, as shown in Fig. 6c. Fig. 6d shows that the peak from PTFE remained after many cycles, demonstrating stability of PTFE in cathode. The new peak at 684.4 eV was attributed to PF_6^- from electrolyte decomposition.

The cycling stability test was performed under 0.5C at room temperature. The ICE of hard carbon is low, which results in reduced energy density of LiBs but could be improved with prelithiation [28]. As shown in Fig. 7a, the ICE of the full cell was close to 100% with the help of prelithiation. The full cells have good stability with more than 95% capacity retention after 50 cycles and 90% capacity retention after 90 cycles, as exhibited in Fig. 7b. The average coulombic efficiency for the first 50 cycles was almost 99.95%, demonstrating the formation of stable solid electrolyte interface.

4. Conclusion

PTFE fibrillation-based SF LFP electrode was successfully fabricated with the help of CNT, where CNT act as conductive additive and matrix to hold LFP particles to ensure further fibrillation of PTFE when pressed through calendering machine. The SF LFP electrode demonstrated good stability and better rate capability than SC counterparts because of good conductivity of CNT and spot contact between PTFE fibrils and LFP particles. With the help of prelithiation, the ICE of SF LFP/hard carbon cells was increased to 100% and showed decent cycling stability under the current of 1.5 mA/cm^2 with more than 95% capacity retention after 50 cycles. The simple fabrication procedure and good performance of SF LFP/hard carbon cells makes it promising to replace current SC procedure for commercial LiBs.

CRediT authorship contribution statement

Yang Zhang: Methodology, Investigation, Writing – original draft, Writing – review & editing, Visualization. **Song Lu:** Investigation, Writing – review & editing. **Fengliu Lou:** Investigation, Formal analysis, Supervision, Writing – review & editing. **Zhixin Yu:** Conceptualization, Methodology, Validation, Resources, Supervision, Writing – review & editing.

Declaration of Competing Interest

The authors declare that they have no known competing financial interests or personal relationships that could have appeared to influence the work reported in this paper.

Data availability

Data will be made available on request.

Acknowledgement

The authors would like to thank the Norwegian Research Council and Beyonder AS for the financial support of this project under project No. 310353.

Supplementary materials

Supplementary material associated with this article can be found, in the online version, at doi:10.1016/j.electacta.2023.142469.

References

[1] M.S. Whittingham, Ultimate limits to intercalation reactions for lithium batteries, Chem. Rev. 114 (2014) 11414–11443.
[2] W. Chen, J. Liang, Z. Yang, G. Li, A review of lithium-ion battery for electric vehicle applications and beyond, Energy Procedia 158 (2019) 4363–4368.
[3] K. Laadjal, A.J.M. Cardoso, Estimation of lithium-ion batteries state-condition in electric vehicle applications: issues and state of the art, Electronics (Basel) 10 (2021) 1588.
[4] S. Matteson, E. Williams, Learning dependent subsidies for lithium-ion electric vehicle batteries, Technol. Forecast. Soc. Change 92 (2015) 322–331.
[5] J. Li, Z. Du, R.E. Ruther, S.J. An, L.A. David, K. Hays, M. Wood, N.D. Phillip, Y. Sheng, C. Mao, Toward low-cost, high-energy density, and high-power density lithium-ion batteries, Jom 69 (2017) 1484–1496.
[6] H.-H. Ryu, H.H. Sun, S.-T. Myung, C.S. Yoon, Y.-K. Sun, Reducing cobalt from lithium-ion batteries for the electric vehicle era, Energy Environ. Sci. 14 (2021) 844–852.
[7] W.B. Hawley, J. Li, Electrode manufacturing for lithium-ion batteries—analysis of current and next generation processing, J. Energy Storage 25 (2019), 100862.
[8] H. Liu, X. Cheng, Y. Chong, H. Yuan, J.-Q. Huang, Q. Zhang, Advanced electrode processing of lithium ion batteries: a review of powder technology in battery fabrication, Particuology 57 (2021) 56–71.
[9] D.L. Wood, J.D. Quass, J. Li, S. Ahmed, D. Ventola, C. Daniel, Technical and economic analysis of solvent-based lithium-ion electrode drying with water and NMP, Drying Technol. 36 (2018) 234–244.
[10] M. Wang, X. Dong, I.C. Escobar, Y.-T. Cheng, Lithium ion battery electrodes made using dimethyl sulfoxide (DMSO)—a green solvent, ACS Sustain. Chem. Eng. 8 (2020) 11046–11051.
[11] Y. Lu, C.-Z. Zhao, H. Yuan, J.-K. Hu, J.-Q. Huang, Q. Zhang, Dry electrode technology, the rising star in solid-state battery industrialization, Matter 5 (2022) 876–898.
[12] Q. Wu, J.P. Zheng, M. Hendrickson, E.J. Plichta, Dry process for fabricating low cost and high performance electrode for energy storage devices, MRS Adv. 4 (2019) 857–863.
[13] Y. Zhang, S. Lu, F. Lou, Z. Yu, Leveraging synergies by combining polytetrafluorethylene with polyvinylidene fluoride for solvent-free graphite anode fabrication, Energy Technol. 10 (2022), 2200732.
[14] H. Duong, J. Shin, Y. Yudi, Dry electrode coating technology, 48th Power Sources Conference, 2018, pp. 34–37.
[15] F. Hippauf, B. Schumm, S. Doerfler, H. Althues, S. Fujiki, T. Shiratsuchi, T. Tsujimura, Y. Aihara, S. Kaskel, Overcoming binder limitations of sheet-type solid-state cathodes using a solvent-free dry-film approach, Energy Storage Mater. 21 (2019) 390–398.
[16] J. Quan, S. Zhao, D. Song, T. Wang, W. He, G. Li, Comparative life cycle assessment of LFP and NCM batteries including the secondary use and different recycling technologies, Sci. Total Environ. 819 (2022), 153105.
[17] C.S. Ioakimidis, A. Murillo-Marrodán, A. Bagheri, D. Thomas, K.N. Genikomsakis, Life cycle assessment of a lithium iron phosphate (LFP) electric vehicle battery in second life application scenarios, Sustainability 11 (2019) 2527.
[18] S. Chen, G. Zhang, C. Wu, W. Huang, C. Xu, C. Jin, Y. Wu, Z. Jiang, H. Dai, X. Feng, Multi-objective optimization design for a double-direction liquid heating system-based Cell-to-Chassis battery module, Int. J. Heat Mass Transf. 183 (2022), 122184.
[19] T. Altenburg, N. Corrocher, F. Malerba, China's leapfrogging in electromobility. A story of green transformation driving catch-up and competitive advantage, Technol. Forecast. Soc. Change 183 (2022), 121914.
[20] H. Zhou, M. Liu, H. Gao, D. Hou, C. Yu, C. Liu, D. Zhang, J.-C. Wu, J. Yang, D. Chen, Dense integration of solvent-free electrodes for Li-ion supercabattery with boosted low temperature performance, J. Power Sources 473 (2020), 228553.
[21] Y. Zhang, F. Huld, S. Lu, C. Jektvik, F. Lou, Z. Yu, Revisiting polytetrafluorethylene binder for solvent-free lithium-ion battery anode fabrication, Batteries 8 (2022) 57.
[22] J. Blumm, A. Lindemann, M. Meyer, C. Strasser, Characterization of PTFE using advanced thermal analysis techniques, Int. J. Thermophys. 31 (2010) 1919–1927.
[23] V. Villani, A study on the thermal behaviour and structural characteristics of polytetrafluoroethylene, Thermochim. Acta 162 (1990) 189–193.
[24] K. Wang, Y. Xu, H. Wu, R. Yuan, M. Zong, Y. Li, V. Dravid, W. Ai, J. Wu, A hybrid lithium storage mechanism of hard carbon enhances its performance as anodes for lithium-ion batteries, Carbon N Y 178 (2021) 443–450.
[25] L. Xie, C. Tang, Z. Bi, M. Song, Y. Fan, C. Yan, X. Li, F. Su, Q. Zhang, C. Chen, Hard carbon anodes for next-generation Li-ion batteries: review and perspective, Adv. Energy Mater. 11 (2021), 2101650.
[26] N. Ren, L. Wang, X. He, L. Zhang, J. Dong, F. Chen, J. Xiao, B. Pan, C. Chen, High ICE hard carbon anodes for lithium-ion batteries enabled by a high work function, ACS Appl. Mater. Interfaces 13 (2021) 46813–46820.
[27] Y. Shen, J. Qian, H. Yang, F. Zhong, X. Ai, Chemically prelithiated Hard-carbon anode for high power and high capacity Li-ion batteries, Small 16 (2020), 1907602.
[28] X. Su, C. Lin, X. Wang, V.A. Maroni, Y. Ren, C.S. Johnson, W. Lu, A new strategy to mitigate the initial capacity loss of lithium ion batteries, J. Power Sources 324 (2016) 150–157.